

Lyapunov spectrum of chaotic maps with a long-range coupling mediated by a diffusing substance

R. L. Viana · A. M. Batista · C. A. S. Batista ·
K. C. Iarosz

Received: 1 June 2016 / Accepted: 6 October 2016 / Published online: 17 October 2016
© Springer Science+Business Media Dordrecht 2016

Abstract We investigate analytically and numerically coupled lattices of chaotic maps where the interaction is non-local, i.e., each site is coupled to all the other sites but the interaction strength decreases exponentially with the lattice distance. This kind of coupling models an assembly of pointlike chaotic oscillators in which the coupling is mediated by a rapidly diffusing chemical substance. We consider a case of a lattice of Bernoulli maps, for which the Lyapunov spectrum can be analytically computed and also the completely synchronized state of chaotic Ulam maps, for which we derive analytically the Lyapunov spectrum.

Keywords Lyapunov exponents · Coupled map lattices · Long-range coupling

1 Introduction

Spatially extended dynamical systems with finite degrees of freedom have long been used as toy models for the description of continuous systems like fluids and plasmas [1]. A particular type of those systems are coupled map lattices, for which the space and time are discrete variables, but allowing for a continuous state variable [2]. Coupled map lattices are thus more complicated, in the dynamical sense, than cellular automata due to their capacity of generating complex spatio-temporal patterns [3].

Most investigations on coupled map lattices have been focused on the so-called locally coupled lattices, for which each lattice site interacts with its nearest neighbors [2]. This kind of coupling is physically related to diffusion, which is essentially a local phenomenon applicable to systems obeying Fick's law. Indeed, a locally coupled map lattice can describe a reaction–diffusion system for which the reaction occurs at discrete times.

On the other hand, many works have considered globally coupled lattices, in which each site interacts with the mean field generated by all other sites, irrespective of their relative position in the lattice [2]. This kind of network has been first investigated by Winfree in his pioneering works on the synchronization of biological systems [4]. Moreover, the well-known Kuramoto model of coupled oscillators uses this kind of coupling [5], with many physical applications such

R. L. Viana (✉)

Department of Physics, Federal University of Paraná,
Curitiba, Paraná, Brazil
e-mail: viana@fisica.ufpr.br

A. M. Batista

Department of Mathematics, State University of Ponta
Grossa, Ponta Grossa, Paraná, Brazil

C. A. S. Batista

Center for Marine Studies, Federal University of Paraná,
Ponta do Paraná, Paraná, Brazil

K. C. Iarosz

Institute of Physics, University of São Paulo, São Paulo,
São Paulo, SP, Brazil

as Josephson junction arrays [6], semiconductor laser arrays [7], Landau damping of plasmas [8], cortical oscillations [9], and bursting behavior of neurons [10].

It turns out that a globally coupled lattice is non-local since it takes into account the interaction of each site with all its neighbors. However, the lattice distance between them does not play any role, what can be considered a kind of approximation. In general, non-local couplings would need to consider the lattice distance between them. One physically interesting model for that was proposed by Kuramoto, who considered the coupling among spatially localized oscillators mediated through a diffusing chemical substance [11–13]. In this model, each oscillator secretes a chemical with a rate proportional to the oscillator dynamics, and this chemical diffuses in the medium, its local concentration affecting the dynamics of the oscillators themselves. When the diffusion is much faster than the oscillator period, the local concentration of the mediator chemical relaxes to a stationary value, and the coupling intensity among oscillators decreases with their lattice distance in an exponential way for one-dimensional lattices. This diffusion-mediated coupling model has been used to describe bursting synchronization in neuronal networks [14] and circadian rhythms in the suprachiasmatic nucleus [15].

In spite of its importance in the description of a number of biologically relevant phenomena, there are relatively few studies on the dynamics of diffusion-mediated coupled map lattices. One of the basic quantities that can be computed in such systems is the Lyapunov spectrum, from which other quantities of interest can be extracted like the Kolmogorov-Sinai entropy and the Lyapunov dimension [16]. More often, the calculation of the Lyapunov exponents can be made only numerically, but in some cases, it can be performed analytically, what has been done for non-local coupled map lattices for which the coupling strength decreases with the lattice distance as a power law [17–20]. Two cases can be considered for this task: (i) when the map is piecewise linear (constant slope) and (ii) when there is complete synchronization of all sites.

The goal of this paper is to compute the Lyapunov spectrum for these cases, namely lattices of chaotic maps (Bernoulli) with diffusion-mediated coupling and complete synchronization in lattices of chaotic maps (logistic, Ulam-type maps). In the latter case, the Lyapunov spectrum can be used to predict the critical cou-

pling strength for the transition to synchronization that is numerically observed. Recently, González-Avella and Anteneodo [21] computed the largest Lyapunov exponent to characterize the chaoticity of delayed coupled maps with adjustable range of interactions. There are studies in which the maximal Lyapunov exponent was considered as a diagnostic tool in a network of Fermi-Pasta-Ulam model where the coupling decays as the distance [22] and in Hamiltonian systems with long-range interactions [23]. In addition, Laffargue et al. [24] presented large-scale fluctuations of the largest Lyapunov exponent in spatially extended systems that describe diffusive fluctuation hydrodynamics.

This paper is organized as follows: in Sect. 2, we outline the Kuramoto model for the diffusion-mediated coupling of maps. Section 3 considers the Lyapunov spectrum of a lattice of Bernoulli (piecewise linear) maps. In Sect. 4, we investigate the completely synchronized state of a coupled logistic map (Ulam) lattice with diffusion-mediated coupling, the result being used for investigate the transition to synchronization as the coupling strength is varied through a critical value. The last section is devoted to our Conclusions.

2 Diffusion-mediated coupling model

Since we deal with spatially extended systems, it is necessary to introduce two different classes of vectors, represented with a different notation: (i) positions \vec{r} in a d -dimensional Euclidean space, to which the sites belong; (ii) state variables $\mathbf{X}_n = (x_{1n}, x_{2n}, \dots, x_{Mn})^T$ in a M -dimensional phase space of the dynamical variables characterizing the state of each system at a given discrete time n . Hence, we have N pointlike sites located at discrete positions \vec{r}_i , where $i = 1, 2, \dots, N$, in the d -dimensional Euclidean space; and $\mathbf{X}_n^{(i)}$ is the state variable for the i th site at time n , whose time evolution is governed by the map $\mathbf{M}(\mathbf{X}^{(i)})$ (see Fig. 1).

In this work, we will deal for simplicity with a one-dimensional system whose state variable is denoted simply by $x_n^{(i)}$, and whose dynamics is governed by a map $x \mapsto f(x)$. We suppose that the dynamics in each site is affected by the local concentration of a chemical, denoted as $A(\vec{r}, n)$, through a coupling function g :

$$x_{n+1}^{(i)} = f(x_n^{(i)}) + g(A(\vec{r}_i, n)), \quad (1)$$

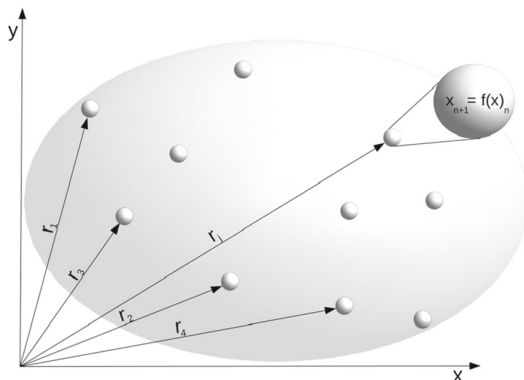


Fig. 1 Schematic figure of the Kuramoto’s model of chemical coupling among oscillators

whereas the chemical concentration satisfies a diffusion equation of the form

$$\epsilon \frac{\partial A}{\partial n} = -\eta A + D \nabla^2 A + \sum_{j=1}^N h(x_n^{(j)}) \delta(\vec{r} - \vec{r}_j), \quad (2)$$

where $\epsilon \ll 1$ is a small parameter representing the fact that diffusion occurs in a timescale faster than the intrinsic period of individual sites, η is a phenomenological damping parameter (representing the chemical degradation of the mediating substance), and D is a diffusion coefficient. The diffusion equation above has a source term h which depends on the state of individual sites located at \vec{r}_i , since each site is supposed to release a chemical with a rate depending on the current value of its own state variable.

We assume, as in Ref. [5], that the diffusion is so fast, compared with the period characteristic of each site, that we may set $\epsilon \dot{A} = 0$ such that the concentration relaxes to a stationary value that can be written in the following form:

$$A(\vec{r}_i) = \sum_{j=1}^N \sigma(\vec{r}_i - \vec{r}_j) h(x_n^{(j)}), \quad (3)$$

where $\sigma(\vec{r}_i - \vec{r}_j)$ is a Green function, which is the solution of

$$(\eta - D \nabla^2) \sigma(\vec{r}_i - \vec{r}) = \delta(\vec{r}_i). \quad (4)$$

On substituting Eq. (3) into Eq. (2) we obtain an equation expressing chemical coupling in the adiabatic approximation

$$x_{n+1}^{(i)} = f(x_n^{(i)}) + g \left(\sum_{j=1}^N \sigma(\vec{r}_i - \vec{r}_j) h(x_n^{(j)}) \right). \quad (5)$$

If g is a linear function of the state variable for each site, we write

$$x_{n+1}^{(i)} = f(x_n^{(i)}) + \sum_{j=1}^N \sigma(\vec{r}_i - \vec{r}_j) g(h(x_n^{(j)})). \quad (6)$$

We will choose the following form for the coupling function:

$$g(h(x_n^{(j)})) = \begin{cases} \epsilon f(x_n^{(j)}), & \text{if } j \neq i, \\ -\epsilon f(x_n^{(i)}), & \text{if } j = i, \end{cases} \quad (7)$$

which corresponds to the so-called future coupling, in that each coupled map remains in the same range as for the isolated map, and where $\epsilon > 0$ is a coupling strength. Inserting (7) into (8) yields

$$x_{n+1}^{(i)} = (1 - \epsilon) f(x_n^{(i)}) + \epsilon \sum_{j=1}^N \sigma(\vec{r}_i - \vec{r}_j) f(x_n^{(j)}). \quad (8)$$

Fourier-transforming Eq. (4), the interaction kernel is given by (in a d -dimensional physical space)

$$\sigma(\vec{r}_i - \vec{r}) = \frac{1}{(2\pi)^d} \int d^d \vec{q} \frac{e^{i\vec{q} \cdot (\vec{r}_i - \vec{r})}}{\eta + D|\vec{q}|^2}. \quad (9)$$

If the coupling is isotropic (in the absence of a diffusion flow, for example), the kernel is a function of $r_{ij} = |\vec{r}_i - \vec{r}_j|$ and can be expressed as

$$\sigma(r_{ij}) = C \begin{cases} \exp(-\gamma r_{ij}), & \text{if } d = 1, \\ K_0(\gamma r_{ij}), & \text{if } d = 2, \\ \frac{\exp(-\gamma r_{ij})}{\gamma r_{ij}}, & \text{if } d = 3, \end{cases} \quad (10)$$

where K_0 is the modified Bessel function of the second kind and order 0, the constant γ is the inverse of the coupling length and is given by

$$\gamma = \sqrt{\frac{\eta}{D}}, \tag{11}$$

and the constant C is determined from the normalization condition

$$\int d^d \vec{r} \sigma(\vec{r}) = 1. \tag{12}$$

Let us adhere to the one-dimensional case, for which we work in a regular lattice parameterized by the spatial length z and with constant spacing Δ , in such a way that $x_n^{(i)} = x(z = i\Delta)$, with $i = 1, 2, \dots, N$. Hence, the non-locally coupled map lattice reads

$$x_{n+1}^{(i)} = (1 - \varepsilon) f(x_n^{(i)}) + \varepsilon C \sum_{j=1}^N e^{-\gamma \Delta r_{ij}} f(x_n^{(j)}), \tag{13}$$

where the constant C is determined from the normalization condition (12), which now reads

$$\sum_{j=1}^N \sigma(|\vec{r}_j - \vec{r}|) = 1, \tag{14}$$

such that

$$C = \left[2 \sum_{j=1}^N e^{-\gamma \Delta r_{ij}} \right]^{-1}. \tag{15}$$

Without loss of generality, we will make $\Delta = 1$ from now on.

We will use periodic boundary conditions:

$$x_n^{(i \pm N)} = x_n^{(i)}, \quad (i = 1, 2, \dots, N), \tag{16}$$

in such a way that the distance between two lattice sites is the less of the two possibilities:

$$r_{ij} = \min_{\ell} |i - j + \ell N|. \tag{17}$$

In this case, it is more convenient to change the summation index in the coupling term of (13) in a more symmetric form:

$$x_{n+1}^{(i)} = (1 - \varepsilon) f(x_n^{(i)}) + \frac{\varepsilon}{\kappa(\gamma)} \sum_{s=1}^{N'} e^{-\gamma s} \left[f(x_n^{(i-s)}) + f(x_n^{(i+s)}) \right], \tag{18}$$

where the normalization factor has been written in the form

$$\kappa(\gamma) = 2 \sum_{s=1}^{N'} e^{-\gamma s}, \tag{19}$$

where $N' = (N - 1)/2$ for N odd.

It is instructive to explore the limiting cases of this form of coupling. If γ goes to zero then $\kappa(0) = 2N' = N - 1$ and we have a global (all-to-all) type of coupling

$$x_{n+1}^{(i)} = (1 - \varepsilon) f(x_n^{(i)}) + \frac{\varepsilon}{N - 1} \sum_{s=1, s \neq i}^N f(x_n^{(s)}). \tag{20}$$

In the limit of large γ , the exponential factor decays very rapidly with the lattice distance ℓ , such that only the term with $\ell = 1$ contributes significantly to the summations, yielding $\kappa(\infty) = 2e^{-\gamma}$ and the coupling term takes into account only the nearest neighbors of a given site

$$x_{n+1}^{(i)} = (1 - \varepsilon) f(x_n^{(i)}) + \frac{\varepsilon}{2} \left[f(x_n^{(i-1)}) + f(x_n^{(i+1)}) \right], \tag{21}$$

which is the well-known local (diffusive or Laplacian) coupling. Hence, depending on the value of the inverse coupling length, we can pass continuously from a global to a local coupling type.

3 Lyapunov exponents

The coupled map lattice with N sites is a dynamical system in a N -dimensional phase space, which can be formally written as

$$\mathbf{x}_{n+1} = \mathbf{F}(\mathbf{x}_n), \tag{22}$$

where the state vector can be written as $\mathbf{x}_n = (x_n^{(1)}, x_n^{(2)}, \dots, x_n^{(N)})^T$. Let the corresponding tangent

vector be written as $\xi_n = (\delta x_n^{(1)}, \delta x_n^{(2)}, \dots, \delta x_n^{(N)})^T$. On linearizing Eq. (22), we obtain the tangent map

$$\xi_{n+1} = \mathbf{DF}(\mathbf{x}_n)\xi_n, \tag{23}$$

where $\mathbf{DF}(\mathbf{x}_n) \equiv \mathbf{T}_n$ is the jacobian matrix of Eq. (22), with components

$$T_n^{(ij)} = \frac{\partial x_{n+1}^{(i)}}{\partial x_n^{(j)}}. \tag{24}$$

Starting from an initial displacement ξ_0 , we iterate Eq. (23) n times and obtain

$$\xi_n = \tau_n \xi_0, \tag{25}$$

where we have defined the ordered product of jacobian matrices:

$$\tau_n = \mathbf{T}_{n-1}\mathbf{T}_{n-2}\dots\mathbf{T}_1\mathbf{T}_0. \tag{26}$$

Defining the matrix

$$\hat{\Lambda} = \lim_{n \rightarrow \infty} (\tau_n^T \tau_n)^{1/2n}, \tag{27}$$

with eigenvalues $\{\Lambda_k\}_{k=1}^N$, the Lyapunov exponents of the coupled map lattice (22) are obtained as

$$\lambda_k = \ln \Lambda_k, \quad (k = 1, 2, \dots, N). \tag{28}$$

If the Lyapunov exponents are ordered, the corresponding spectrum is denoted by $\{\tilde{\lambda}_k\}_{k=1}^N$.

In the non-locally coupled map lattice given by Eq. (18), a standard calculation shows that the elements of the jacobian matrix are given by

$$T_n^{(ik)} = (1 - \varepsilon)f'(x_n^{(i)})\delta_{ik} + \frac{\varepsilon}{\kappa(\gamma)} \exp(-\gamma r_{ik}) f'(x_n^{(k)}) (1 - \delta_{ik}), \tag{29}$$

where the primes denote differentiation of the map function with respect to its argument. Let us define a symmetric matrix \mathbf{B} with elements

$$B_{ik} = e^{-\gamma r_{ik}} (1 - \delta_{ik}), \tag{30}$$

and, in terms of them, another matrix

$$\hat{\mathbf{B}}^{(ik)} = (1 - \varepsilon)\delta_{ik} + \frac{\varepsilon}{\kappa(\gamma)} B_{ik}. \tag{31}$$

Using the latter, we can write the jacobian matrix in (29) as

$$\mathbf{T}_n = \hat{\mathbf{B}}\mathbf{D}_n = \left[(1 - \varepsilon)\mathbf{1} + \frac{\varepsilon}{\kappa(\gamma)} \mathbf{B} \right] \mathbf{D}_n, \tag{32}$$

where the jacobian of uncoupled maps is a diagonal matrix:

$$D_n^{(ik)} = f'(x_n^{(i)})\delta_{ik}. \tag{33}$$

4 Lyapunov spectrum of Bernoulli maps

Let x be a variable defined in the unit interval $[0, 1)$. The so-called Bernoulli map is

$$x_{n+1} = f(x_n) = \beta x, \quad (\text{mod } 1), \tag{34}$$

which, for $\beta > 1$, is strongly chaotic (transitive). In fact, its Lyapunov exponent is $\lambda = \ln \beta > 0$. In the case $\beta = 2$, we have the well-known baker transformation, which is equivalent to a bilateral shift operator of a bi-infinite two-state symbolic sequence [25]. Moreover, the baker transformation is topologically conjugate to the horseshoe map [26].

Since $f'(x) = \beta$ there follows that

$$\mathbf{D}_n = \beta \mathbf{I}, \quad \mathbf{T}_n = \beta \hat{\mathbf{B}}, \quad \tau_n = \beta^n \hat{\mathbf{B}}^n, \quad \hat{\Lambda} = \beta \hat{\mathbf{B}}.$$

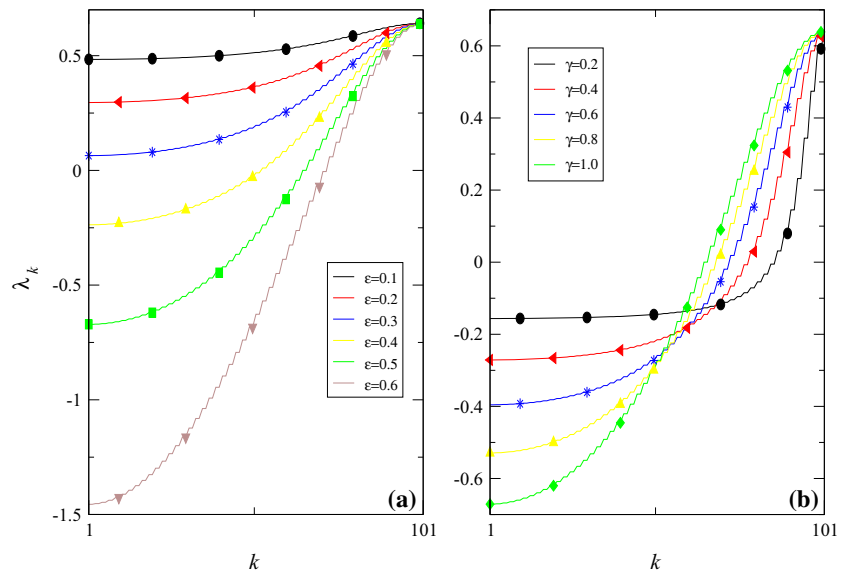
If $\{b_k\}_{k=1}^N$ are the eigenvalues of \mathbf{B} , then for the matrix $\hat{\mathbf{B}}$ the corresponding eigenvalues are given by

$$\hat{b}_k = (1 - \varepsilon) + \frac{\varepsilon}{\kappa(\gamma)} b_k, \quad (k = 1, 2, \dots, N), \tag{35}$$

such that the eigenvalues of $\hat{\Lambda}$ are $\Lambda_k = \beta \hat{b}_k$. Due to the periodic boundary conditions (16), the matrix \mathbf{B} is circulant and its diagonal elements are identically zero since such terms were ruled out when computing the coupling part of the jacobian matrix. A standard matrix calculation using Fourier transform yields

$$b_k = 2 \sum_{m=1}^{N'} e^{-\gamma m} \cos\left(\frac{2\pi km}{N}\right), \quad (k = 1, 2, \dots, N) \tag{36}$$

Fig. 2 Lyapunov spectrum of a one-dimensional lattice of $N = 101$ Bernoulli maps with $\beta = 1.9$ and chemical coupling with $\alpha = 1.0$ and various values of the coupling constant; **a** $\varepsilon = 0.5$ and various values of the coupling range for illustrative purposes



in terms of them the Lyapunov exponents of the coupled Bernoulli map lattice read

$$\lambda_k = \ln \beta + \ln \left| (1 - \varepsilon) + \frac{\varepsilon}{\kappa(\gamma)} b_k \right|. \tag{37}$$

Let us consider the two limiting cases of the above expression. For $\gamma = 0$, global type of coupling, the spectrum reads

$$\lambda_k = \ln \beta + \ln \left| (1 - \varepsilon) + \frac{2\varepsilon}{N-1} \sum_{m=1}^{N'} \cos \left(\frac{2\pi km}{N} \right) \right|. \tag{38}$$

Using Lagrange’s identity for the sum of cosines there follows that

$$\lambda_k = \ln \beta + \ln \left| (1 - \varepsilon) + \frac{\varepsilon}{N-1} \left[-1 + \frac{\sin(k\pi)}{\sin \left(\frac{k\pi}{N} \right)} \right] \right|. \tag{39}$$

If $k \neq N$, we have the same exponents, a $(N - 1)$ -fold symmetry:

$$\lambda_k = \ln \beta + \ln \left| 1 - \varepsilon \frac{N}{N-1} \right|, \tag{40}$$

whereas if $k = N$, the exponent is simply $\lambda_N = \ln \beta$. These results are in accordance with previous findings [27].

The $\gamma \rightarrow \infty$ case brings about the locally coupled lattice, for which the spectrum (37) yields

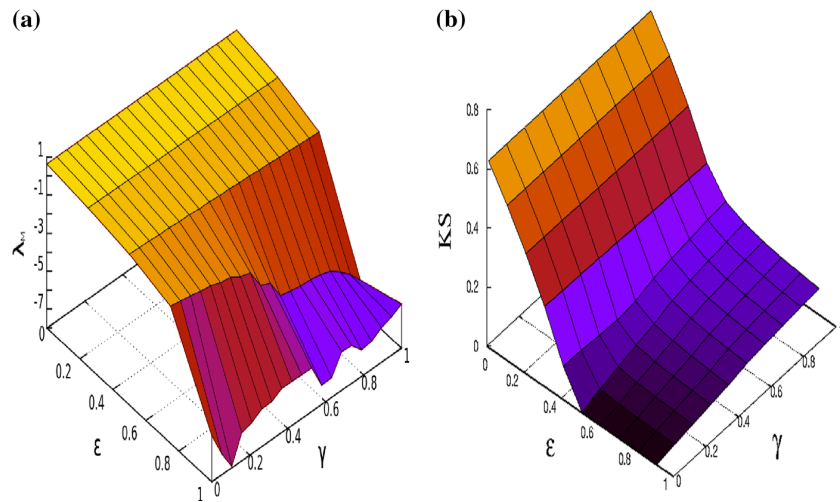
$$\lambda_k = \ln \beta + \ln \left| 1 - 2\varepsilon \sin^2 \left(\frac{\pi k}{N} \right) \right|. \tag{41}$$

which also has been already found by Kaneko [28].

Now let us consider the intermediate case of $\gamma = 1.0$ and a chain of $N = 101$ coupled Bernoulli maps with $\beta = 1.9$. In Fig. 2a, we plot the (ordered) Lyapunov spectrum λ_k versus k for coupling range $\gamma = 1.0$ and different values of the coupling constant ε . The curves were obtained from Eq. (37), whereas the indicated points refer to numerically obtained values of the Lyapunov exponent for selected sites. In the latter case, we computed the Lyapunov spectrum directly from the definition, computing the product of jacobian matrices and its eigenvalues, using balancing, reduction to the Hessenberg form and QR-algorithm [29]. We computed only a few sites so as not to eclipse the agreement between the analytical and numerical expressions.

In Fig. 2a, it is clearly seen that the maximum Lyapunov exponent is $\ln \beta = 0.6418$, corresponding to the uncoupled maps (for this reason it is independent of ε). The spectrum of Lyapunov exponents is monotonic and its minimum decreases as ε increases. For $\varepsilon \lesssim 0.3$

Fig. 3 **a** Smallest Lyapunov exponent and **b** Density of KS-entropy as a function of the coupling strength and range, for a lattice of $N = 501$ chaotic Bernoulli maps with $\beta = 1.9$



(below the blue line in the figure), all the exponents are positive, whereas part of them become negative as ε increases further.

The Lyapunov spectrum for fixed $\varepsilon = 0.5$ and varying γ is shown in Fig. 2b. It is interesting that, as γ decreases, approaching the global coupling limit, the spectrum becomes almost degenerate for around half of the sites, mirroring the full degeneracy observed when $\gamma = 0$.

The relative contribution of the positive Lyapunov exponents to the entire spectrum can be quantified by the density of Kolmogorov-Sinai (KS) entropy. For systems having a Sinai-Ruelle-Bowen (SRB) measure, the latter is given by [30,31]

$$h = \langle \lambda_j \rangle_{j, \lambda_j > 0} = \frac{1}{N} \sum_{j=1}^{\lambda_j > 0} \lambda_j. \tag{42}$$

We used the analytical expression (37) in order to select the positive ones and apply Eq. (42) to obtain the smallest Lyapunov exponent and the KS-entropy density shown in Fig. 3a, b, respectively, as a function of coupling strength and range. In this Figure, we consider $N = 501$ for illustrative purposes; however, in Sect. 6, we will show results with varying lattice size.

In the global case ($\gamma = 0$), we have a clear-cut transition to chaos, as the value of h increases suddenly from zero to positive values, as ε decreases past a critical value $\varepsilon_c \approx 0.5$. In fact, thanks to the quasi-total degeneracy of the Lyapunov spectrum for this case [see

Eq. (40)], we deduce that all exponents will be positive if

$$\varepsilon \leq \frac{N-1}{N} \left(1 - \frac{1}{\beta}\right), \quad \varepsilon \geq \frac{N-1}{N} \left(1 + \frac{1}{\beta}\right), \tag{43}$$

a condition that, for the same parameters used in Fig 3, namely $\beta = 1.9$ and $N = 501$, amounts to $\varepsilon \leq \varepsilon_c = 0.4727$ and $\varepsilon \geq 1.5229$ (the latter case is not depicted in Fig. 3). Moreover, for the intervals (43), it turns out that the density of KS-entropy is

$$h = \ln \beta + \left(\frac{N-1}{N}\right) \ln \left|1 - \varepsilon \frac{N}{N-1}\right|. \tag{44}$$

If ε is small enough, an approximate result is obtained as a power series

$$h \approx \ln \left\{ \beta \left[1 - \varepsilon - \frac{1}{2(N-1)} \varepsilon^2 + o(\varepsilon^3) \right] \right\}. \tag{45}$$

By way of contrast, in the local case (γ large), the spectrum (41) indicates that, for small coupling strength, all exponents are positive, such that the entropy is as large as it is in the global case, a fact evident in Fig. 3. The (non-ordered) Lyapunov spectrum for small values of ε have typically positive values, starting from $k = 1$ and N , for which the exponents are $\ln \beta$, and with the lowest value at $k = N/2$. The spectrum has a symmetry with respect to this value.

The value of $\lambda_{N/2}$ is positive provided either of the inequalities below are fulfilled

$$\begin{aligned} \varepsilon &< \frac{1}{2} \left(1 - \frac{1}{\beta}\right) = 0.23684, \\ \varepsilon &> \frac{1}{2} \left(1 + \frac{1}{\beta}\right) = 0.76315. \end{aligned} \tag{46}$$

As ε grows further, this exponent becomes negative, as well as a number of other ones with different values of β . Nevertheless, even if ε is large enough, a certain number of exponents remain positive.

Another quantity of interest which we can compute from the Lyapunov spectrum is the Lyapunov dimension D of the attractor for the coupled map lattice in its N -dimensional phase space. Let p be the largest integer for which $\sum_{j=1}^p \lambda_j \geq 0$. Then D is defined by one of the following relations [32]

$$D = \begin{cases} 0 & \text{if there is no such } p \\ p + \frac{1}{|\lambda_{p+1}|} \sum_{j=1}^p \lambda_j & \text{if } p < N \\ N & \text{if } p = N \end{cases} \tag{47}$$

It has been conjectured that the Lyapunov dimension provides an estimate for the information dimension of the attractor, which is in general less than its capacity dimension.

Figure 4 shows the values of D as a function of the coupling parameters. A cursory look at both Figs. 3 and 4 shows a resemblance between them, which comes from the similar definitions in the case of many posi-

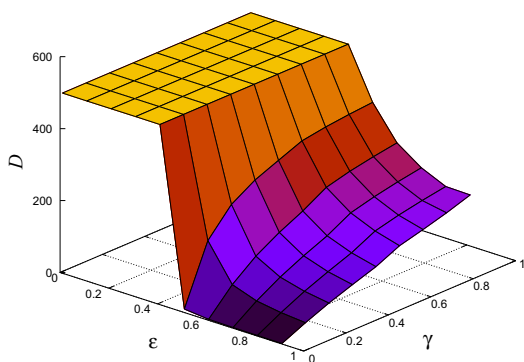


Fig. 4 Lyapunov dimension as a function of the coupling strength and range, for a lattice of $N = 501$ chaotic Bernoulli maps with $\beta = 1.9$

tive Lyapunov exponents, the difference being the normalization used in each case. In particular, for weakly coupled maps, the system attractor has practically the same dimension as the phase space itself (N) due to the many positive exponents.

As the coupling strength grows, however, a number of these exponents turns negative producing synchronization and, as we will see in the next Section, a drastic reduction in the attractor dimensionality. In the extreme case in which all maps are synchronized the dimension reduces to the unity (which is the dimension of the uncoupled systems).

5 Lyapunov spectrum of the completely synchronized state

More than 25 years ago, it was discovered that two or more chaotic systems, despite having the characteristic sensitive dependence to initial conditions, can synchronize their chaotic evolutions [33,34]. Since then this subject has developed into a subfield of nonlinear dynamics with various applications in physical and biological systems [35].

We define a completely synchronized state of the coupled map lattice in the following way

$$x_n^{(1)} = x_n^{(2)} = \dots = x_n^{(N)} = x_n^*, \tag{48}$$

for all times. If we substitute this expression into (18), we find an identity, showing that a completely synchronized state is a valid solution as long as the maps are identical.

Geometrically, Eq. (48) defines a one-dimensional synchronization manifold \mathcal{S} in the N -dimensional phase space of the coupled lattice. The remaining $(N - 1)$ directions are transversal to \mathcal{S} . We shall denote the Lyapunov exponents of the completely synchronized state as $\{\tilde{\lambda}_k^*\}_{k=1}^N$. From the definition (48), we can derive the following quantities for the completely synchronized state of one-dimensional maps

$$\mathbf{D}_n = f'(x_n^*)\mathbf{I}, \quad \mathbf{T}_n = f'(x_n^*)\hat{\mathbf{B}}, \tag{49}$$

$$\tau_n = \prod_{j=0}^{n-1} f'(x_j^*)\hat{\mathbf{B}}, \quad \hat{\Lambda} = \lim_{n \rightarrow \infty} \left[\prod_{j=0}^{n-1} f'(x_j^*) \right]^{1/n} \hat{\mathbf{B}}. \tag{50}$$

As in the previous case, the eigenvalues of the matrix $\hat{\mathbf{B}}$ are given by (35), in such a way that the eigenvalues of the matrix $\hat{\mathbf{A}}$ read

$$\Lambda_k = \lim_{n \rightarrow \infty} \left(\prod_{j=0}^{n-1} f'(x_j^*) \right)^{1/n} \hat{b}_k, \tag{51}$$

and, taking the natural logarithm, we obtain the Lyapunov exponents corresponding to the completely synchronized state

$$\lambda_k^* = \lim_{n \rightarrow \infty} \frac{1}{n} \sum_{j=0}^{n-1} \ln |f'(x_j^*)| + \ln \left| (1 - \varepsilon) + \frac{\varepsilon}{\kappa(\gamma)} b_k \right|, \tag{52}$$

where b_k are given from (36).

The uncoupled maps are supposed to be strongly chaotic, and the ergodic property is shown to hold [25]. However, the ergodicity of a coupled chaotic map lattice, although not rigorously proved, can be assumed to hold for weak enough coupling. As a matter of fact, the existence of a SRB measure has been proved for a few coupled map lattices only [36]. Assuming ergodicity, we can replace the time average in (54) by an average over the attractor of uncoupled maps:

$$\begin{aligned} & \lim_{n \rightarrow \infty} \frac{1}{n} \sum_{j=0}^{n-1} \ln |f'(x_j^*)| \\ &= \int_a^b dx^* \rho(x^*) \ln |f'(x_j^*)| = \lambda_U, \end{aligned} \tag{53}$$

where $\lambda_U > 0$ is the Lyapunov exponent of an uncoupled map, and $\rho(x^*)$ is the invariant density of iterations on the interval $[a, b]$ for the chaotic map f . Substituting (53) and (36) into (54) there results that

$$\begin{aligned} \lambda_k^* &= \lambda_U + \ln \left| (1 - \varepsilon) + \frac{2\varepsilon}{\kappa(\gamma)} \right. \\ & \left. \sum_{m=1}^{N'} e^{-\gamma m} \cos \left(\frac{2\pi km}{N} \right) \right|, \quad (k = 1, 2, \dots, N). \end{aligned} \tag{54}$$

In the following, we shall consider the Ulam map, defined in the interval $x \in [0, 1)$

$$x_{n+1} = f(x_n) = 4x_n(1 - x_n), \tag{55}$$

which is the logistic map for $a = 4$. The initial conditions $x_0^{(i)}, i = 1, 2, \dots, N$ are randomly chosen in the interval $[0, 1)$. Due to its topological conjugacy to the baker transformation, in this case the invariant density is known to be [25]

$$\rho(x) = \frac{1}{\pi \sqrt{x(1-x)}}, \tag{56}$$

such that its Lyapunov exponent is, according (53),

$$\lambda_U = \frac{1}{\pi} \int_0^1 \frac{\ln |4(1-2x^*)|}{\sqrt{x^*(1-x^*)}} dx^* = \ln 2. \tag{57}$$

6 Transversal stability of the completely synchronized state

The completely synchronized state can only be observed in numerical computation if the synchronization manifold \mathcal{S} is stable with respect to all the transversal directions. The dynamics on \mathcal{S} is the same as the uncoupled maps. If the latter are chaotic, the maximal exponent is positive ($\tilde{\lambda}_1^* > 0$, for $\tilde{\lambda}_k^*$ stands for the ordered spectrum). The remaining $(N - 1)$ exponents are related to transverse directions with respect to \mathcal{S} .

Hence, the completely synchronized state is transversely stable if $\tilde{\lambda}_2^* \leq 0$, i.e., the manifold \mathcal{S} loses transversal stability when the largest transversal exponent is zero. Some authors call this transition a blowout bifurcation [37]. If $\tilde{\lambda}_2^* > 0$, the synchronized state is transversely unstable and, in practice, cannot be achieved for typical initial conditions, since any initial condition off- \mathcal{S} will generate a trajectory which does not converge to the synchronized state.

Note that in the Lyapunov spectrum (54) $\tilde{\lambda}_2^*$ corresponds to $k = 1$ (or $k = N - 1$ due to the two-fold degeneracy) and $k = N'$ (or $k = N' + 1$ for the same reason). Hence,

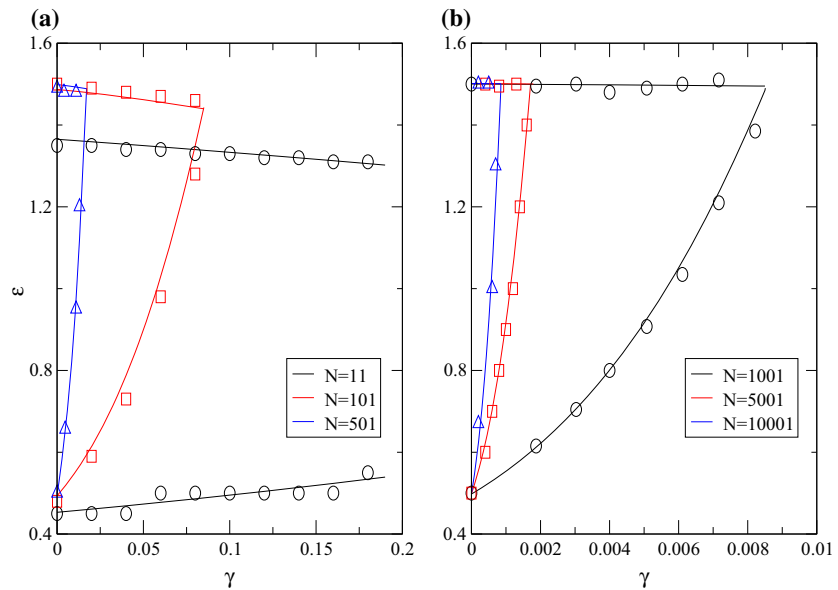
$$\lambda_2^* = \lambda_U + \ln \left| (1 - \varepsilon) + \frac{\varepsilon}{\kappa(\gamma)} b_{1,N'} \right|, \tag{58}$$

where

$$b_1 = 2 \sum_{m=1}^{N'} e^{-\gamma m} \cos \left(\frac{2\pi m}{N} \right), \tag{59}$$

$$b_{N'} = 2 \sum_{m=1}^{N'} e^{-\gamma m} \cos \left(\frac{\pi(N-1)m}{N} \right). \tag{60}$$

Fig. 5 Critical lines for completely synchronization of chaotic maps in the parameter plane of coupling strength ε versus coupling range γ , for different lattice sizes. The curves were obtained using the analytical result given by Eq. (64), whereas the symbols stand for numerical results using the order parameter computed from Eq. (70). The region of transversely stable states shrinks with increasing γ



Using (58), the condition for transversal stability of the completely synchronized state is that the coupling constant lies in the interval (for given values of γ and N):

$$\varepsilon_c \leq \varepsilon \leq \varepsilon'_c, \tag{61}$$

where

$$\varepsilon_c = (1 - e^{-\lambda v}) \left(1 - \frac{b_1}{\kappa(\gamma)} \right)^{-1}, \tag{62}$$

$$\varepsilon'_c = (1 + e^{-\lambda v}) \left(1 - \frac{b_{N'}}{\kappa(\gamma)} \right)^{-1}. \tag{63}$$

Let us now consider the Ulam map. In this case, the critical values of the coupling constant given by (62) and (63) are, respectively

$$\varepsilon_c = \frac{1}{2\Delta}, \quad \varepsilon'_c = \frac{3}{2\Delta'}, \tag{64}$$

where

$$\Delta = 1 - \frac{b_1}{\kappa(\gamma)}, \quad \Delta' = 1 - \frac{b_{N'}}{\kappa(\gamma)}. \tag{65}$$

In Fig. 5a, b we plot the critical curves for the transition to a completely synchronized state in the parameter plane of coupling strength ε versus the coupling range

γ for a coupled Ulam map lattice with various values of the lattice size N , using the analytical formulae above. The region in-between the curves for ε_c and ε'_c corresponds to a transversely stable synchronized state.

We observe a strong dependence on the lattice size N : For large N , the upper value of ε'_c is almost constant at ~ 1.5 , whereas the lower ε_c increases monotonically with γ until it crosses the upper curve. For γ higher than this crossing value, there is no region for transversely stable synchronized state, i.e., it ceases to be observed numerically. Practically, we thus say that the lattice cannot be synchronized at all. This crossing value is observed to decrease with increasing N ; hence, it is worthwhile to consider the thermodynamical limit of the lattice ($N \rightarrow \infty$).

This analysis is easier to be performed in the globally coupled case ($\gamma = 0$), for which $\kappa = N - 1$ and

$$b_1 = -1, \tag{66}$$

$$b_{N'} = -1 + \frac{\sin \frac{\pi(N-1)}{2}}{\sin \frac{\pi(N-1)}{2N}}, \tag{67}$$

such that (64) and (65) yield

$$\varepsilon_c = \frac{N - 1}{2N}, \tag{68}$$

$$\varepsilon'_c = \frac{3(N - 1)}{2N}. \tag{69}$$

In the limit, $N \rightarrow \infty$ we have that $\varepsilon_c = 1/2$ and $\varepsilon'_c = 3/2$, in accordance with Eq. (62).

In order to check these analytical results, we resort to a numerical diagnostic of phase synchronization, which is the complex order parameter introduced by Kuramoto [11–13]

$$z(t) = R(t)e^{i\varphi(t)} = \frac{1}{N} \sum_{j=1}^N e^{i\theta_j(t)}. \tag{70}$$

The quantities R and $\varphi \in [0, 2\pi)$ are, respectively, the amplitude and angle of a gyrating vector which is equal to the vector sum of phasors for each oscillator in a one-dimensional lattice with periodic boundary conditions. In order to see the meaning of $z(t)$, let us analyze two limits cases. Firstly, for a completely phase-synchronized state, the order parameter magnitude is $R(t) = 1$ for all times. In the second place, let us consider a completely non-synchronized pattern, for which the phases are so spatially uncorrelated that they can be considered as randomly distributed over $[0, 2\pi)$. The order parameter in this case has zero magnitude, since it is a space-average over randomly distributed variables.

In general, the order parameter magnitude fluctuates in time, so we usually compute its time average, after transients have died out. In our simulations, we have discarded 5000 iterations to eliminate transient behavior. The symbols in Fig. 5 stand for numerically obtained values of the critical values of ε and γ for which there is a transition to a completely synchronized state, i.e., the symbols mark the parameter values for which the (time-averaged) order parameter magnitude R either increases from zero or decreases from the unity. The numerical results using the order parameter agree with the analytical predictions based on the Lyapunov spectrum for all parameter values considered.

A similar coupling prescription uses a power-law spatial dependence $\sim r^{-\alpha}$, instead of an exponential decay as here, and it was used to discuss many dynamical aspects of non-local coupled maps, like shadowing breakdown [38], spatial correlations [39], and unstable dimension variability [40]. The coupled map lattice with that prescription would read

$$x_{n+1}^{(i)} = (1 - \varepsilon) f(x_n^{(i)}) + \frac{\varepsilon}{\eta(\alpha)} \sum_{s=1}^{N'} s^{-\alpha} \left[f(x_n^{(i-s)}) + f(x_n^{(i+s)}) \right], \tag{71}$$

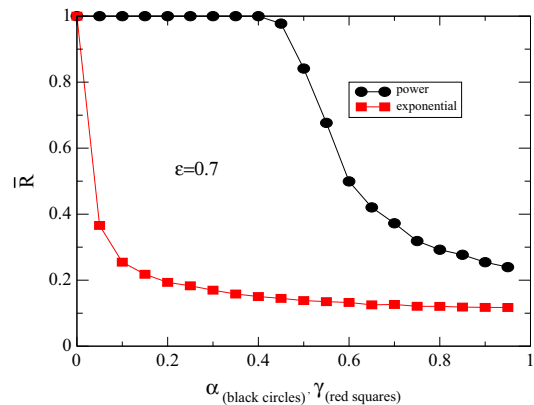


Fig. 6 Average order parameter for the power-law (black circles) and exponential (red squares) coupling models, for $\varepsilon = 0.7$. (Color figure online)

where the normalization factor is now

$$\eta(\alpha) = 2 \sum_{s=1}^{N'} s^{-\alpha}, \tag{72}$$

with $N' = (N - 1)/2$, as before.

In order to compare the power-law coupling prescription with the exponential model here considered, in Fig. 6, we show the variation of the time-averaged order parameter for the power-law (black circles) and exponential (red squares) coupling models as a function of α and γ , respectively, by keeping $\varepsilon = 0.7$. For $\alpha = \gamma = 0$, both prescriptions stand for a global (all-to-all) coupling, and thus we expect that the lattice is completely synchronized for ε large enough. However, as both α and κ decrease, the decay of \bar{R} is faster for the exponential coupling, with respect to the power-law coupling. For example, if $\kappa = 0.4$, the power-law coupling leads to an almost synchronized lattice, whereas $\alpha = 0.4$ already results in a non-synchronized state. As both parameters increase further, both prescriptions tend to exhibit similar behavior.

7 Conclusions

A non-local type of coupling between dynamical systems in a spatial lattice can be obtained by considering the interaction of the system units being mediated by a chemical which is both secreted and absorbed by the systems, the corresponding rates being affected by the

system local dynamics. The mediating chemical diffuses along the space in which the systems are embedded. If the diffusion timescale is fast compared with the typical period of the local dynamics, we can neglect the time dependence and consider the stationary limit of the chemical concentration. In one spatial dimension, this leads to a coupling between systems whose intensity decreases exponentially with the lattice distance. The coupling is characterized by two parameters: the strength ε and range γ , in such a way that we can pass from a global type of coupling, when $\gamma = 0$, to a local one (large γ). This kind of coupling can be used to investigate a variety of dynamical behavior, e.g., the existence of chimeras (spatially inhomogeneous states) and the transition to completely synchronized states.

We have obtained the Lyapunov exponents for a coupled map lattice in one spatial dimension, with analytical expressions for the particular case of Bernoulli (piecewise linear) chaotic maps. Our general expression agrees with the previously known cases of local and global coupling. This information was used to compute the density of KS-entropy and Lyapunov dimension of the system. Another application was the investigation of the transversal stability of the completely synchronized state of a coupled chaotic map lattice. For one-dimensional maps, the synchronization manifold is likewise one-dimensional, and the second largest Lyapunov exponent (out of the ordered spectrum) gives the transversal stability of the synchronized state. From knowledge of the general expression, it was thus possible to estimate the thresholds (in the coupling parameter plane) of the synchronization transition for a lattice of coupled Ulam maps. The analytical results agree with the numerical results from direct evaluation of the Lyapunov spectrum.

The Lyapunov spectrum provides, by means of the second largest Lyapunov exponent, the parameter values for which there is a completely synchronized state. Therefore, the determination of regions of chaos synchronization, in the coupling parameter space, is a useful application of Lyapunov exponent analysis. Analytical results, when available, are important due to the difficulties involved in the analytical characterization of chaoticity in dynamical systems. In this work, we show that Lyapunov exponents can be analytically obtained for coupled Bernoulli maps. We have used coupled Bernoulli maps because they are piecewise linear, and the derivative of the isolated map does not depend on the state variable, what enables us to per-

form the analytical computations in an exact form. In this way, we believe that this work can be useful for other maps belonging to the same class. Considering coupled Ulam maps with a long-range coupling, it is possible to find analytically the Lyapunov spectrum. We used coupled Ulam maps to illustrate the synchronization of chaos because they present strong chaos. As a future work, this method can be applied to other non-local interactions.

Acknowledgements This work was made possible with the partial financial support of the following Brazilian government agencies: CNPq, CAPES, FAPESP (Grant 2016/16148-5), and Fundação Araucária (State of Paraná).

References

1. Kaneko, K., Tsuda, I.: *Complex Systems: Chaos and Beyond: A Constructive Approach with Applications*. Springer, Berlin (2001)
2. Chazottes, J.-R., Fernandez, B. (eds.): *Dynamics of Coupled Map Lattices and of Related Spatially Extended Systems*. Springer, Berlin (2005)
3. Mitchel, M.: *Complexity: A Guided Tour*. Oxford University Press, Oxford (2009)
4. Murray, J.D.: *Mathematical Biology*, vol. 1, 3rd edn. Springer, Berlin (2002)
5. Acebrón, J.A., Bonilla, L.L., Vicente, C.J.P., Ritort, F., Spigler, R.: The Kuramoto model: a simple paradigm for synchronization phenomena. *Rev. Mod. Phys.* **77**, 137 (2005)
6. Wiesenfeld, K., Colet, P., Strogatz, S.H.: Frequency locking in Josephson arrays: connection with the Kuramoto model. *Phys. Rev. E* **57**, 1563 (1998)
7. Kozyreff, G., Vladimirov, A.G., Mandel, P.: Global coupling with time delay in an array of semiconductor lasers. *Phys. Rev. Lett.* **85**, 3809 (2000)
8. Strogatz, S.H., Mirollo, R.E., Matthews, P.C.: Coupled nonlinear oscillators below the synchronization threshold: relaxation by generalized Landau damping. *Phys. Rev. Lett.* **68**, 2730 (1992)
9. Breakspear, M., Heitmann, S., Daffertshofer, A.: Generative models of cortical oscillations: neurobiological implications of the Kuramoto model. *Front. Hum. Neurosci.* **4**, 190 (2010)
10. Ferrari, F.A.S., Viana, R.L., Lopes, S.R., Stoop, R.: Phase synchronization of coupled bursting neurons and the generalized Kuramoto model. *Neural Netw.* **66**, 107 (2015)
11. Kuramoto, Y.: Scaling behavior of turbulent oscillators with non-local interaction. *Prog. Theor. Phys.* **94**, 321–330 (1995)
12. Kuramoto, Y., Nakao, H.: Origin of power-law spatial correlations in distributed oscillators and maps with nonlocal coupling. *Phys. Rev. Lett.* **76**, 4352 (1996)
13. Kuramoto, Y., Nakao, H.: Power-law spatial correlations and the onset of individual motions in self-oscillatory media with non-local coupling. *Physica D* **103**, 294–313 (1997)
14. Viana, R.L., Batista, A.M., Batista, C.A.S., de Pontes, J.C.A., Silva, F.A.S., Lopes, S.R.: Bursting synchronization

- in networks with long-range coupling mediated by a diffusing chemical substance. *Commun. Nonlinear Sci. Numer. Simul.* **17**, 2924–2942 (2012)
15. Silva, F.A.S., Lopes, S.R., Viana, R.L.: Synchronization of biological clock cells with a coupling mediated by the local concentration of a diffusing substance. *Commun. Nonlinear Sci. Numer. Simul.* **35**, 37–52 (2016)
 16. Batista, A.M., Viana, R.L.: Kolmogorov-Sinai entropy for locally coupled piecewise linear maps. *Phys. A* **308**, 125–134 (2002)
 17. Anteneodo, C., Pinto, S.E.S., Batista, A.M., Viana, R.L.: Analytical results for coupled-map lattices with long-range interactions. *Phys. Rev. E* **68**, 045202 (2003)
 18. Anteneodo, C., Batista, A.M., Viana, R.L.: Chaos synchronization in long-range coupled map lattices. *Phys. Lett. A* **326**, 227–233 (2004)
 19. Batista, A.M., Viana, R.L.: Lyapunov exponents of a lattice of chaotic maps with a power law coupling. *Phys. Lett. A* **286**, 134 (2001)
 20. dos Santos, A.M., Woellner, C.F., Lopes, S.R., Batista, A.M., Viana, R.L.: Lyapunov spectrum of a lattice of chaotic systems with local and non-local couplings. *Chaos. Solit. Fract.* **32**, 702 (2007)
 21. González-Avella, J.C., Anteneodo, C.: Complete synchronization equivalence in asynchronous and delayed coupled maps. *Phys. Rev. E* **93**, 052230 (2016)
 22. Bagchi, D., Tsallis, C.: Sensitivity to initial conditions of a d -dimensional long-range-interaction quartic Fermi-Pasta-Ulam model: Universal scaling. *Phys. Rev. E* **93**, 062213 (2016)
 23. Christodoulidi, H., Bountis, T., Drossos, L.: Numerical integration of variational equations for Hamiltonian systems with long range interactions. *Appl. Numer. Math.* **104**, 158 (2016)
 24. Laffargue, T., Sollich, P., Tailleur, J., van Wijland, F.: Large-scale fluctuations of the largest Lyapunov exponent in diffusive systems. *Europhys. Lett.* **110**, 10006 (2015)
 25. Devaney, R.L.: *An Introduction to Chaotic Dynamical Systems*. Benjamin-Cummings Publishing Co, San Francisco (1986)
 26. Guckenheimer, J., Holmes, P.: *Nonlinear Oscillations, Dynamical Systems, and Bifurcations of Vector Fields*. Springer, New York (1983)
 27. Kaneko, K.: Clustering, coding, switching, hierarchical ordering, and control in a network of chaotic elements. *Phys. D* **41**, 137 (1990)
 28. Kaneko, K.: Pattern dynamics in spatiotemporal chaos: pattern selection, diffusion of defect and pattern competition intermittency. *Phys. D.* **34**, 1–41 (1989)
 29. Press, W.H., Teukolsky, S.A., Vetterling, W.T., Flannery, B.P.: *Numerical Recipes in C: The art of scientific computing*. University Press, Cambridge (1992)
 30. Pesin, Ya B.: Characteristic Lyapunov exponents and smooth ergodic theory. *Russ. Math. Surv.* **32**, 55–114 (1977)
 31. Ruelle, D.: An inequality for the entropy of differentiable maps. *Bol. Soc. Bras. Mat.* **9**, 83–87 (1978)
 32. Ott, E.: *Chaos in Dynamical Systems*. University Press, Cambridge (1994)
 33. Fujisaka, H., Yamada, T.: Stability theory of synchronized motion in coupled-oscillator systems. *Prog. Theor. Phys.* **69**, 32–47 (1982)
 34. Pecora, L.M., Carroll, T.L.: Synchronization in chaotic systems. *Phys. Rev. Lett.* **64**, 821 (1990)
 35. Pikovsky, A., Rosenblum, M., Kurths, J.: *Synchronization: A Universal Concept in Nonlinear Sciences*. University Press, Cambridge (2001)
 36. Bricmont, J., Kupiainen, A.: Infinite-dimensional SRB measures. *Phys. D* **103**, 18–33 (1997)
 37. Nagai, Y., Lai, Y.-C.: Periodic-orbit theory of the blowout bifurcation. *Phys. Rev. E* **56**, 4031 (1997)
 38. Viana, R.L., Grebogi, C., Pinto, S.E.S., Lopes, S.R., Batista, A.M., Kurths, J.: Bubbling bifurcations: loss of synchronization and shadowing breakdown in complex systems. *Phys. D* **206**, 94 (2005)
 39. Vasconcelos, D.B., Viana, R.L., Lopes, S.R., Batista, A.M., Pinto, S.E.S.: Spatial correlations and synchronization in coupled map lattices with long-range interactions. *Phys. A* **343**, 201 (2004)
 40. Viana, R.L., Grebogi, C., Pinto, S.E.S., Lopes, S.R., Batista, A.M., Kurths, J.: Validity of numerical trajectories in the synchronization transition of complex systems. *Phys. Rev. E* **68**, 067204 (2003)